

Threshold resummation for W -boson pair production at NNLO+NNLL

Pulak Banerjee,^a Chinmoy Dey,^b M. C. Kumar^b and Vaibhav Pandey^b

^a*Istituto Nazionale di Fisica Nucleare, Gruppo collegato di Cosenza, I-87036 Arcavacata di Rende, Cosenza, Italy*

^b*Department of Physics, Indian Institute of Technology Guwahati, Guwahati-781039, India*

E-mail: pulak.banerjee@lnf.infn.it, d.chinmoy@iitg.ac.in,
mckumar@iitg.ac.in, vphiitg@iitg.ac.in

ABSTRACT: We present results for threshold resummation of the invariant mass distribution, for on-shell production of a pair of W -bosons at next-to-next-to-leading order + next-to-next-to-leading logarithmic (NNLO+NNLL) accuracy in QCD. Owing to its sensitivity to the self-interactions between gauge bosons, this process is important to investigate at the energies of the Large Hadron Collider (LHC). We achieve this resummation by exploiting the factorization properties of the soft and virtual parts of the partonic cross-section. Our analysis has been carried out for the invariant mass distribution up to $Q = 2500$ GeV. At this highest Q we find that, for 13.6 TeV LHC, the NNLL resummation enhances the NNLO cross-sections by about 6.3% and reduces the conventional scale uncertainties from 6.8% at NNLO to 4.1% at NNLO+NNLL. We also estimate the intrinsic uncertainties due to the non-perturbative parton distribution functions at the highest perturbative order, for both fixed-order and resummed results, to be around 3% for $Q \sim 2000$ GeV.

KEYWORDS: Resummation, perturbative QCD, LHC

Contents

1	Introduction	1
2	Theoretical Framework	3
3	Numerical Results	7
4	Summary	13
A	Resummation coefficients	14

1 Introduction

The Standard Model(SM) of particle physics has been successful in explaining intricacies inherent in the world around us, like the electron’s magnetic moment, discovery of the Higgs boson [1, 2]. Yet it has many shortcomings, for example the origin of dark matter, matter-antimatter asymmetry in our universe, to name a few. Stringent limits have been put on physics beyond the Standard Model. Production of an intermediate charged particle X (predicted mass range between 300 and 2000 GeV), decaying to a W boson and a photon has been studied and no significant excess above the predicted background has been found [3]. Similarly, no new physics in high-mass diphoton events has also not been observed [4]. Search for pair production of mass-degenerate Higgsinos has been conducted at the Large Hadron Collider(LHC) and no evidence has been observed [5]. Over the last decade, the LHC has precisely measured many fundamental parameters of the SM. One of the finest examples is the precise measurement of the W boson mass at the CMS [6]. The importance of such precise measurements lies in the fact that any deviation from the SM value can signal the presence of beyond the SM(BSM) physics. For example, BSM physics could modify the W boson mass via quantum loop effects [7]. Precise SM theoretical predictions from the perturbative side have played a major role in W boson mass measurements. [6].

It becomes important to precisely calculate observables in SM, up to high accuracy in perturbation theory. The production of a pair of massive gauge bosons at the LHC is an important process that has been studied extensively, both theoretically and experimentally. The process can also be used for testing the SM electroweak symmetry-breaking mechanism as well as in the study of fundamental weak interactions among elementary particles. This process is important, owing to the large cross-section for W^+W^- (henceforth we call it W -boson pair) as compared to ZZ or W^+Z process, coupled with the inherent challenge in the final state mass reconstruction. Measurement of the W -boson pair production cross-sections has been done at CMS [8] as well as at ATLAS [9]. Significant progress has been made from the theoretical side, too. The leading order cross-section was calculated

decades ago [10]. The next-to-leading order(NLO) corrections for this process were reported in [11, 12]. The helicity amplitudes at the NLO level[13] have enabled the calculation of the total production cross-section [14]. The NLO results, including the full lepton decay correlations in the narrow-width approximation, can be found in [15]. The NLO corrections for W -boson pair in association with 1-jet was performed in [16–19]; for 2-jet results see [20, 21]; for 3-jets the results are available in [22]. Inclusion of resummation effects at next-to-next-to leading log(NNLL) along with NLO corrections, for transverse momentum has been presented in [23–25]. For jet-veto resummation see [26]. Electroweak effects have been studied in [27–29]. For an effective field theory analysis at NLO, see [30, 31]. Polarisation fractions of massive gauge bosons serve as an important test of the symmetry-breaking mechanism in the SM. Polarised W -boson pair production at NLO and NNLO QCD is available in [32] and [33] respectively.

Precision studies entail going beyond NLO. The inclusive production of a on-shell W -boson pair in NNLO QCD was done in [34], where the residual perturbative uncertainty was at 3%. The NNLO helicity amplitudes for two off-shell bosons was calculated in [35, 36]. The NNLO fiducial cross-sections and distributions for W -bosons pair are available [37] decaying to four leptons. The leptonic decays lead to a decrease of the total cross-section as compared to the on-shell W -boson pair production. Upon including NLO EW corrections along with NNLO QCD, precise predictions are available [38]. For fiducial cross-sections(σ) at $\sqrt{s} = 13$ TeV, the NLO EW corrections for W -boson pair production is about -2.1% compared to LO; $\sigma_{\text{NNLO QCD+NLO EW}}$ is about - 1.2% compared to NNLO QCD; $\sigma_{\text{NNLO QCD} \otimes \text{NLO EW}}$ is about -2% compared to NNLO QCD. For differential distributions, at $Q = 1000$ GeV, the cross-sections for NNLO QCD \otimes NLO EW and NNLO QCD + NLO EW are about -5% compared to NNLO QCD [38]. Planar master integrals at NNLO for W -boson pair production via top quark loop, in quark-antiquark annihilation channel, are now available [39]. The loop induced gluon-fusion contributions which starts at $\mathcal{O}(\alpha_s^2)$ at LO are also known [40–43]. Two-loop helicity amplitudes for production of two off-shell vector bosons via gluon-fusion are available [44, 45], which were later used to calculate the full NLO QCD corrections to $gg \rightarrow W^+W^-$ process [46].

Significant progress has also been made in resumming large logarithmic contributions that arise in corner regions of phase space. The transverse momentum resummation at NNLO+NNLL for a vector-boson pair was achieved in [47], where the dominant soft-gluon contributions at small p_T have been resummed to all orders in perturbation theory. Resummation for on-shell W -boson pair production with a jet-veto up to partial N³LL + NNLO accuracy has been studied [48]. The logarithms resummed were the ratio of the transverse momentum of the vetoed-jet and the invariant mass of the final state. Threshold resummation at NNLL supplemented with approximate NNLO results has been investigated in [49]. Using a SCET formalism, the authors have shown that the scale uncertainties (for invariant mass up to 500 GeV) are smaller than the corresponding fixed order ones, upon inclusion of threshold logarithms. Parton shower analysis at NNLO for W -boson pair production has been studied in [50, 51]; using a jet veto, resummation within the SCET approach has been done in [52].

Currently fixed-order invariant mass distributions have been reported till around 1000

GeV [52]. These cross-sections suffer from scale uncertainties arising from unphysical renormalization and factorization scales. If we set these scales to be the same and vary them between $(Q/2, 2Q)$ where Q is the invariant mass of the final state on-shell W -boson pair, we observe that for $Q \sim 500$ GeV, the uncertainty is about 2%. However, for $Q = 2500$ GeV, this scale uncertainty rises to about 6.8%. A major programme of calculating higher-order corrections lies in reducing these scale uncertainties. These high Q regions can be important in searches for signals beyond the SM [3, 4]. The CMS has invariant mass distribution measured up to 1000 GeV region for ZZ production [53]. With the upcoming HL-LHC, the integrated luminosity is expected to reach $3000 - 4000 \text{ fb}^{-1}$, which may allow more events in this TeV region with more statistical data. For the planned FCC-hh [54], the increase in parton fluxes along with the integrated luminosity of $20 - 30 \text{ ab}^{-1}$ can enhance the invariant mass distributions by a few orders of magnitude. A similar kind of situation related to the measurement in high Q regions was also seen in the Drell-Yan process. One of the earliest measurements by CDF, for the Drell-Yan differential cross-section, was done till 1000 GeV [55]. A decade later, CMS reported invariant mass distribution up to 600 GeV while comparing to the theoretical predictions [56], followed by ATLAS measurement till 1500 GeV [57]. Currently, the Drell-Yan invariant mass is measured up to 3000 GeV [58]. The residual theoretical scale uncertainty is about 0.1% at $\text{N}^3\text{LO} + \text{N}^3\text{LL}$ accuracy, for $Q = 3000$ GeV [59]. One of the main motivations of the present work is to minimise the theoretical uncertainties that are as large as 6.8% in the high invariant mass region. After performing the resummation, the seven-point scale uncertainties in the NNLO fixed-order results are found to be reduced for the high invariant mass region to as low as 4.1%. Together with the fixed-order distributions, our resummed results give an estimate of the missing higher-order contributions. It is to be noted that the resummation for on-shell ZZ production process up to NNLO+NNLL has recently been done in [60].

Our paper is organised as follows: in sec 2 we discuss the theoretical framework for the NNLL resummation to the $q\bar{q}$ initiated W -boson pair production process. In sec 3, we discuss our results, and we conclude in sec 4.

2 Theoretical Framework

The hadronic cross-section for W -boson pair production can be written in terms of its partonic counterpart as:

$$\frac{d\sigma}{dQ} = \sum_{a,b=\{q,\bar{q},g\}} \int_0^1 dx_1 \int_0^1 dx_2 f_a(x_1, \mu_F^2) f_b(x_2, \mu_F^2) \int_0^1 dz \delta(\tau - zx_1x_2) \frac{d\hat{\sigma}_{ab}}{dQ}, \quad (2.1)$$

where Q is the invariant mass of the pair of W -bosons. The hadronic and partonic threshold variables τ and z are defined as

$$\tau = \frac{Q^2}{S}, \quad z = \frac{Q^2}{s}, \quad (2.2)$$

where S and s are the hadronic and partonic center of mass energies, respectively. Thus, τ and z are related by $\tau = x_1x_2z$. The calculational framework that we follow is the same

as in [60]. The leading order parton level process has the generic form

$$q(p_1) + \bar{q}(p_2) \rightarrow W^+(p_3) + W^-(p_4). \quad (2.3)$$

We define kinematical variables s, t and u through,

$$(p_1 + p_2)^2 = s, \quad (p_1 - p_3)^2 = t, \quad (p_2 - p_3)^2 = u \quad \text{and} \quad s + t + u = 2m_w^2, \quad (2.4)$$

where, m_w is the mass of the W-boson. We also define x, y and z dimensionless scaling variables as,

$$x = \frac{1-b}{1+b}, \quad y = -\frac{t}{m_w^2}, \quad z = -\frac{u}{m_w^2} \quad (2.5)$$

where, $b = \sqrt{1 - 4m_w^2/s}$. The leading-order (LO) cross-section $\hat{\sigma}_{q\bar{q}}^{(0)}$ for W-boson pair production can be written as,

$$\frac{d\hat{\sigma}_{q\bar{q}}^{(0)}}{dQ} = \frac{1}{2s} \int d\text{PS}_2 \mathcal{M}_{(0,0)}, \quad (2.6)$$

where $d\text{PS}_2$ is the 2-body integral measure and $\mathcal{M}_{(0,0)}$ is the born amplitude, which for the up quark initiated process is given below,

$$\mathcal{M}_{(0,0)} = B_f N (c_{tt}^u \mathcal{F}_0^u - c_{ts}^u \mathcal{J}_0^u + c_{ss}^u \mathcal{K}_0^u). \quad (2.7)$$

Here,

$$\begin{aligned} \mathcal{F}_0^u(x, y) = & \frac{4}{xy^2} \left[(-4x + 4y + 4x^2y + 4y^2 + 3xy^2 + 4x^2y^2 + y^3 + x^2y^3 - xy^4) \right. \\ & + \epsilon \{ 8x - 8y - 8x^2y - 4y^2 - 4x^2y^2 \} \\ & \left. + \epsilon^2 \{ 4y + 4x^2y - 4x(1 + y^2) \} \right], \end{aligned} \quad (2.8)$$

$$\begin{aligned} \mathcal{J}_0^u(x, y) = & \frac{1}{x^2y} \left[4m_w^2(y(4 + y) + x^4y(4 + y) - 2x^2(10 - 4y + y^2) - x(8 - 11y + y^3) \right. \\ & - x^3(8 - 11y + y^3) + \epsilon \{ -16m_w^2(y + x^4y + x(-2 + 3y) + x^3(-2 + 3y) \\ & \left. - x^2(5 - 2y + y^2)) \} \right], \end{aligned} \quad (2.9)$$

$$\begin{aligned} \mathcal{K}_0^u(x, y) = & \frac{1}{x^3} \left[2m_w^4(4 + y + x^6(4 + y) + x^2(-4 + 11y) + x^4(-4 + 11y) - x(-7 + y^2) \right. \\ & - x^5(-7 + y^2) - 2x^3(13 + 5y^2)) + \epsilon \{ -8m_w^4(1 + 2x + 2x^5 + x^6 \\ & \left. + x^2(-1 + 2y) + x^4(-1 + 2y) - 2x^3(3 + y^2)) \} \right]. \end{aligned} \quad (2.10)$$

where ϵ is the dimensional regularization parameter for dimension $d = 4 - 2\epsilon$. The \mathcal{F} , \mathcal{J} and \mathcal{K} expressions for the d -type quark can be easily written in terms of u -type as,

$$\mathcal{F}_0^d(x, z) = \mathcal{F}_0^u(x, y), \quad \mathcal{J}_0^d(x, z) = -\mathcal{J}_0^u(x, y), \quad \mathcal{K}_0^d(x, z) = \mathcal{K}_0^u(x, y). \quad (2.11)$$

The coefficients c_{tt}, c_{ts} and c_{ss} are,

$$\begin{aligned} c_{tt} &= \frac{e^4}{16 \sin^2 \theta_w}, \\ c_{ts} &= \frac{e^4}{4s \sin \theta_w} \left(\mathcal{Q} + 2e_z g_L \frac{s}{s - m_z^2} \right), \\ c_{ss} &= \frac{e^4}{s^2} \left[\left\{ \mathcal{Q} + e_z (g_L + g_R) \frac{s}{s - m_z^2} \right\}^2 + \left\{ e_z (g_L - g_R) \frac{s}{s - m_z^2} \right\}^2 \right] \end{aligned} \quad (2.12)$$

where, for u -type ($\mathcal{Q} = 2/3$) quark,

$$g_L^u = \frac{1}{2 \sin \theta_w \cos \theta_w} \left\{ \frac{1}{2} - \frac{2}{3} \sin^2 \theta_w \right\}, \quad g_R^u = -\frac{1}{2 \sin \theta_w \cos \theta_w} \left\{ \frac{2}{3} \sin^2 \theta_w \right\} \quad (2.13)$$

and, for d -type ($\mathcal{Q} = -1/3$) quark,

$$g_L^d = \frac{1}{2 \sin \theta_w \cos \theta_w} \left\{ -\frac{1}{2} + \frac{1}{3} \sin^2 \theta_w \right\}, \quad g_R^d = -\frac{1}{2 \sin \theta_w \cos \theta_w} \left\{ \frac{1}{3} \sin^2 \theta_w \right\}. \quad (2.14)$$

Here, $e^2 = 4\pi\alpha$ with α being the fine structure constant, θ_w is the weak mixing angle, $e_z \equiv \cos \theta_w / \sin \theta_w$ and m_z is the mass of Z -boson. In the prefactor of Eq. (2.7), N is the $SU(N)$ color, and $B_f (= 1/4 \times 1/9)$ originates from the average of spin and color configurations. To calculate the amplitudes, we have dealt with γ_5 in d -dimensions using Larin's prescription [61].

At higher orders in QCD, the partonic cross-section receives quantum corrections from virtual loops and real emissions. In the threshold region, defined by the limit $z \rightarrow 1$, the available energy in the partonic center-of-mass frame is almost entirely transferred to the production of the final state system. This leaves minimal phase space for additional parton radiations, making soft-gluon effects particularly significant. The partonic cross-section in terms of z can be written as:

$$\frac{d\hat{\sigma}_{ab}}{dQ} = \frac{d\hat{\sigma}_{ab}^{(0)}}{dQ} \left(\Delta_{ab}^{\text{sv}}(z, \mu_F^2) + \Delta_{ab}^{\text{reg}}(z, \mu_F^2) \right). \quad (2.15)$$

The terms Δ_{ab}^{sv} are universal and depend only on the initial state partons. The SV term encapsulates all singular behaviour in the limit $z \rightarrow 1$ as well as the threshold logarithms. The remaining regular terms, denoted by Δ_{ab}^{reg} , are process-dependent and include logarithmic terms beyond the threshold, as well as the regular terms that are finite in the limit $z \rightarrow 1$. Notably, only quark-antiquark and gluon-gluon initiated channels contribute to the SV term.

The singular structure of the SV component is universal and arises from contributions such as virtual form factors [62–66], mass factorization kernels [67–69], and soft-gluon emissions [70–84]. The process-dependent virtual terms in the threshold limit are proportional to $\delta(1-z)$, whereas the universal terms are proportional to the plus distributions, $\mathcal{D}_i = [\ln^i(1-z)/(1-z)]_+$. These contributions can be resummed to all orders in perturbation theory using Mellin-space techniques, where convolutions of terms become normal products.

In Mellin space, the resummed SV cross-section can be written as:

$$\hat{\sigma}_N^{\text{N}^n\text{LL}} = \int_0^1 dz z^{N-1} \Delta_{ab}^{\text{sv}}(z) \equiv g_0 \exp(\Psi_N^{\text{sv}}), \quad (2.16)$$

where g_0 is independent of the Mellin variable N , and the exponent Ψ_N^{sv} resums the large logarithms $\ln^i N$. Up to next-to-next-to-leading logarithmic (NNLL) accuracy, Ψ_N^{sv} takes the form:

$$\Psi_N^{\text{sv}} = \ln(\bar{N}) g_1(\bar{N}) + g_2(\bar{N}) + a_s g_3(\bar{N}) + \dots, \quad (2.17)$$

with $\bar{N} = N e^{\gamma_E}$. The universal functions g_i are well known and their explicit expressions can be found in [81, 85, 86]. The constant g_0 encodes the non-logarithmic contributions and can be expanded in terms of the strong coupling constant a_s ($= g_s^2/(16\pi^2)$):

$$g_0 = 1 + a_s g_{01} + a_s^2 g_{02} + \dots, \quad (2.18)$$

The coefficients g_{01} and g_{02} are process-dependent and are derived using the method outlined in [87, 88], and their expressions can be found in Appendix A. We have used our in-house FORM [89] routines to compute the one-loop virtual corrections (see Appendix A), which are necessary for obtaining g_{01} . The computation of the g_{02} coefficient, which is essential for NNLL accuracy, involves the two-loop amplitude $\mathcal{M}_{(0,2)}$, which is reconstructed using the VVamp package [36], and the one-loop squared amplitude $\mathcal{M}_{(1,1)}$ is generated with our in-house codes.

The resummed cross-section in z -space can now be obtained by performing the inverse Mellin transformation of the resummed cross-section in Mellin space:

$$\frac{d\sigma^{\text{N}^n\text{LL}}}{dQ} = \frac{d\hat{\sigma}^{(0)}}{dQ} \sum_{a,b \in \{q,\bar{q}\}} \int_{c-i\infty}^{c+i\infty} \frac{dN}{2\pi i} \tau^{-N} f_{a,N}(\mu_F) f_{b,N}(\mu_F) \hat{\sigma}_N^{\text{N}^n\text{LL}}. \quad (2.19)$$

Here, following the minimal prescription [90], we choose the contour of integration in the complex plane to avoid the Landau pole at $N = \exp(1/(2a_s\beta_0) - \gamma_E)$. We set $N = c + x e^{i\phi}$ with $c = 1.9$ and $\phi = 3\pi/4$, as in [91].

The differential cross-section after matching to the fixed-order counterparts is given by:

$$\begin{aligned} \frac{d\sigma^{\text{N}^n\text{LO}+\text{N}^n\text{LL}}}{dQ} &= \frac{d\sigma^{\text{N}^n\text{LO}}}{dQ} + \frac{d\hat{\sigma}^{(0)}}{dQ} \sum_{a,b \in \{q,\bar{q}\}} \int_{c-i\infty}^{c+i\infty} \frac{dN}{2\pi i} \tau^{-N} f_{a,N}(\mu_F) f_{b,N}(\mu_F) \\ &\times \left[\hat{\sigma}_N^{\text{N}^n\text{LL}} - \hat{\sigma}_N^{\text{N}^n\text{LL}} \Big|_{\text{tr}} \right]. \end{aligned} \quad (2.20)$$

Here, $\hat{\sigma}_N^{\text{N}^n\text{LL}} \Big|_{\text{tr}}$ denotes the truncation of the resummed cross-section at the n^{th} order to avoid double counting. Mellin-space PDFs, $f_{a,N}$, are obtained via tools such as QCD-PEGASUS [91], or approximated using z -space PDFs as in [75, 85].

3 Numerical Results

In this section, we study the numerical impact of the threshold resummation for the W -boson pair production process at the LHC. For the numerical calculations, we take the masses of the weak gauge bosons to be $m_z = 91.1876$ GeV and $m_w = 80.385$ GeV, and the Weinberg angle is $\sin^2\theta_w = (1 - m_w^2/m_z^2) = 0.222897$. The fine structure constant is taken to be $\alpha \simeq 1/132.2332$ that corresponds to the weak coupling $G_F = 1.166379 \times 10^{-5}$ GeV $^{-2}$. Unless mentioned otherwise, the default choice of the center mass energy of the incoming protons at the LHC is taken to be 13.6 TeV, and throughout we use NNPDF30 [92] parton distribution functions (PDFs) taken from the LHAPDF [93]. We consider $n_f = 4$ light flavours in our analysis and consider a simple scenario where the diagonal elements in CKM matrix is set to unity (no mixing). Accordingly, the LO, NLO and NNLO cross-sections are obtained by convoluting the corresponding coefficient functions with NNPDF30_lo_as_0118_nf_4, NNPDF30_nlo_as_0118_nf_4 and NNPDF30_nnlo_as_0118_nf_4 PDF sets respectively. Except for the PDF uncertainties, we consider the central set (iset=0) as the default choice in our analysis. The strong coupling constant α_s from the corresponding PDF sets is taken from the LHAPDF routines [93], and it varies order by order in the perturbation theory. All the fixed order calculations in the perturbation theory are obtained from the package MATRIX [94]. The fixed order results from MATRIX up to NLO are compared with those obtained from the MadGraph [95], and they are found to be in very good agreement with each other. Further, the NNLO results for this process that are reported in the literature [96, 97] have been successfully reproduced from the MATRIX before using this package for the rest of the analysis. The resummation results are obtained using the in-house developed numerical code.

The unphysical renormalization and factorization scales are set to the central scale $\mu_R = \mu_F = Q$, where Q is the invariant mass of the W -boson pair, which is the hard scale of the problem under consideration. The scale uncertainties are estimated by varying the unphysical renormalization and factorization scales in the range such that $|\ln(\mu_R/\mu_F)| \leq \ln 2$. The symmetric scale uncertainty, defined as the maximum of the absolute deviation of the cross-section from that obtained with the central/default scale choice, is reported in the present work. To better examine the impact of the higher-order corrections from FO and resummation, we define the following ratios of the cross-sections or differential distributions. Such ratios can be readily used in the experimental analysis focusing on the measurement of the W -boson pair production processes at hadron colliders:

$$K_{ij} = \frac{\sigma_{\text{N}^i\text{LO}}}{\sigma_{\text{N}^j\text{LO}}}, \quad R_{ij} = \frac{\sigma_{\text{N}^i\text{LO}+\text{N}^i\text{LL}}}{\sigma_{\text{N}^j\text{LO}}} \quad \text{and} \quad L_{ij} = \frac{\sigma_{\text{N}^i\text{LO}+\text{N}^i\text{LL}}}{\sigma_{\text{N}^j\text{LO}+\text{N}^j\text{LL}}} \quad \text{with } i, j = 0, 1 \text{ and } 2. \quad (3.1)$$

In Fig. [1], we present the results up to NNLO+NNLL for the invariant mass distribution of the W -boson pair from $2m_w$ to 2500 GeV. It can be noticed that the cross-sections vary over about four orders of magnitude for the range of Q considered here. In the right panel, the corresponding fixed order as well as the resummed K-factors, defined in Eq. (3.1), are presented. The NLO K-factor K_{10} varies very mildly from about 1.31 at $Q = 2m_w$ GeV to about 1.49 at $Q = 2500$ GeV, and remains almost constant from $Q = 500$ GeV

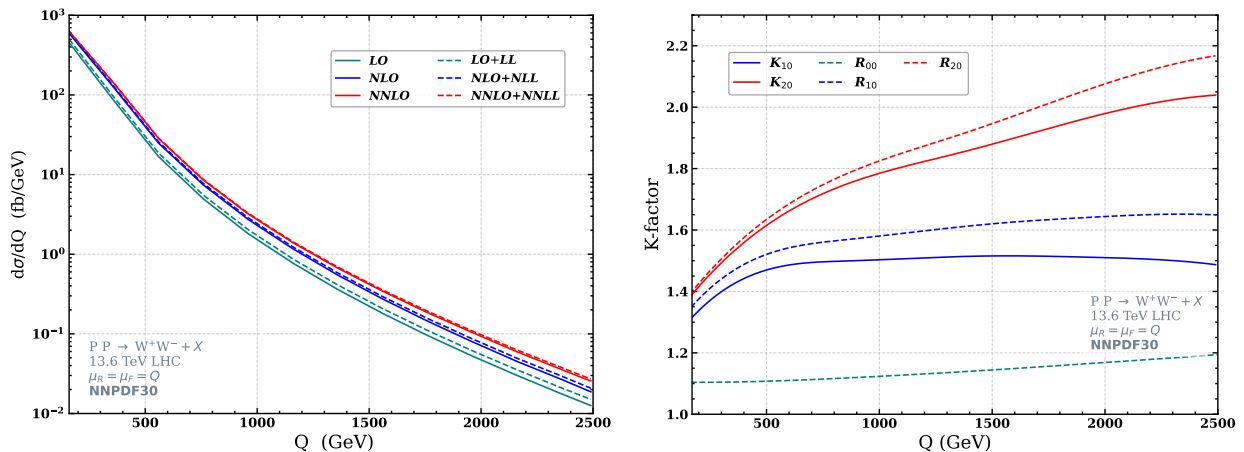


Figure 1. Resummed predictions for the invariant mass distribution (left) of the W -boson pair production and the corresponding K-factors(right) up to NNLO+NNLL.

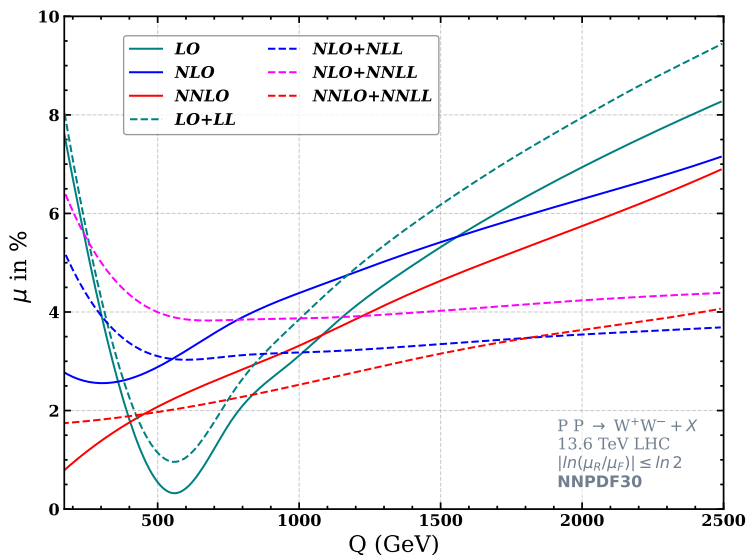


Figure 2. Seven point scale uncertainties for W -boson pair production up to NNLO+NNLL.

to about $Q = 2500$ GeV. In contrast, the NNLO K-factor K_{20} slowly but continuously increases from about 1.38 at $Q = 2m_w$ to about 2.03 for $Q = 2500$ GeV. This clearly shows additional dominant contributions coming from second-order corrections in the higher Q -region, which are due to the presence of sub-processes like $q_1\bar{q}_1 \rightarrow WWq_2\bar{q}_2$. A similar observation can be made for the Z -boson pair production case as well, a more detailed discussion of this kind of contributions can be found in the [38].

In the case of resummed results, we can see from R_{00} that the LL resummation enhances the LO results by about 19% at $Q = 2500$ GeV. While the NLO corrections are 48%, the corresponding NLO+NLL results are about 64% of LO for the same at the same Q value. The corresponding contribution from NNLO is about 103%, whereas the NNLL

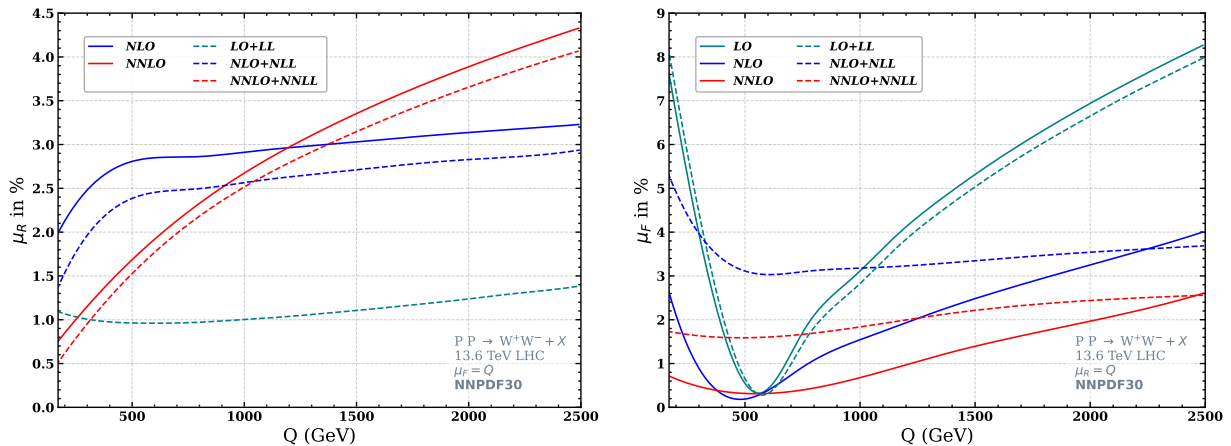


Figure 3. Renormalization(left) and factorization(right) scale uncertainties for W -boson pair production up to NNLO+NNLL.

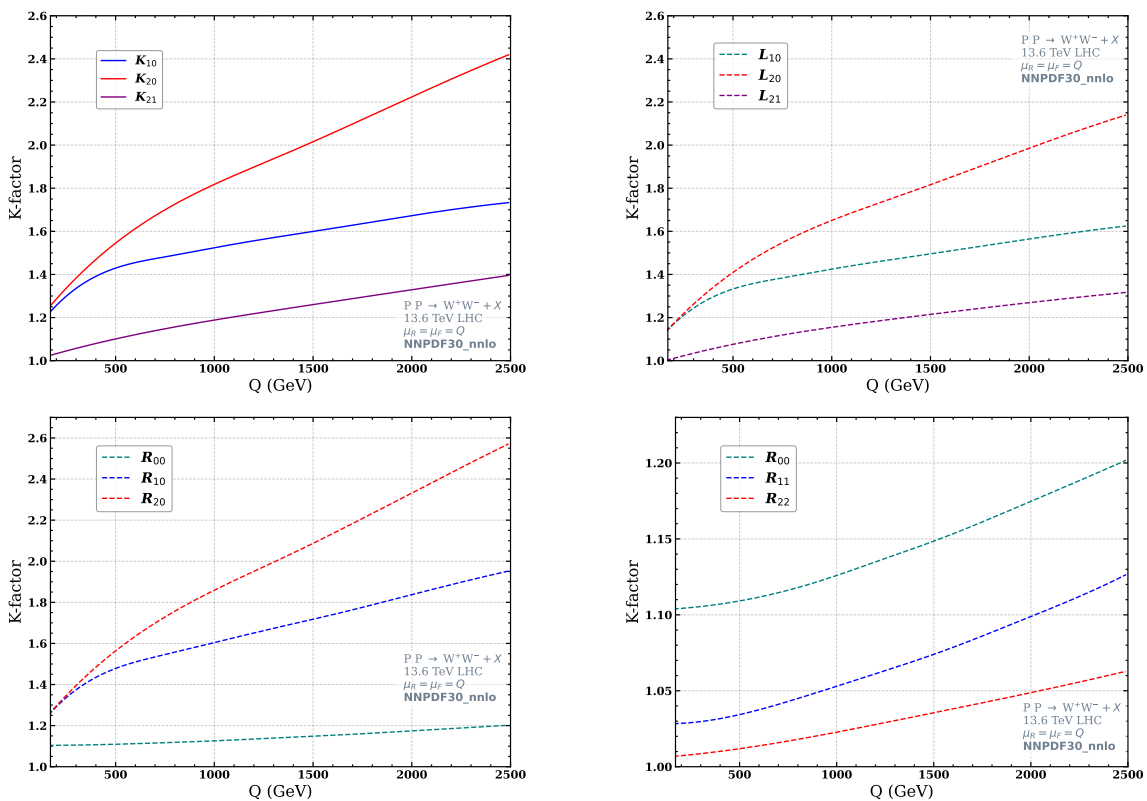


Figure 4. K-factors as defined in Eq. (3.1) but using same NNLO PDFs at various orders in the perturbation theory.

resummation adds an additional 13% of LO, making the R_{20} as large as 2.16 at $Q = 2500$ GeV.

The underlying 7-point theoretical scale uncertainties in the invariant mass distribution up to NNLO+NNLL are presented in Fig. [2]. The maximum uncertainty at $Q = 2m_w$ GeV

for LO is about 7.9%, whereas the inclusion of higher order NLO and NNLO corrections reduces this uncertainty to as low as 2.8% and to less than 0.7%, respectively. The general observation is that these scale uncertainties are found to increase with Q , which for the NNLO case are found to change from about 0.7% at $Q = 2m_w$ to about 6.9% at $Q = 2500$ GeV. Moreover, the scale uncertainties at NNLO are smaller than those at NLO for the entire range of Q considered here, as can be seen from Fig. 2.

In the case of resummed results presented in the Fig. 2, specifically in the low Q -region where the process-dependent regular terms are also dominant (and also because they can not be resummed), the NLL as well as the NNLL resummed results do not show improvement in the scale uncertainties. However, for $Q > 560$ GeV, the resummation of large threshold logarithms results in the reduction of these fixed order scale uncertainties, particularly in the high invariant mass ($Q = 2500$) region. We note here that, as there is no μ_R scale dependence at LO for the process under study, the LO+LL shows enhanced scale uncertainties because of the μ_R scale dependence that enters through LL. This is highlighted in Fig. 3, in the left-hand plot. While for NLO(NNLO), the scale uncertainties reach up to 7.1%(6.8)% at $Q = 2500$ GeV, the corresponding ones at NLO+NLL(NNLO+NNLL) level reduce to 3.7%(4.1%). It is also to be noted that the NLO+NNLL results for this process have been available for quite some time now [49]. However, the inclusion of the NNLO corrections has reduced these 7-point scale uncertainties in NLO+NNLL from about 6.6%(4.0%) at $Q = 2m_w$ ($Q = 550$ GeV) to about 1.7%(2.0%) at NNLO+NNLL level.

In the Fig. [3], we separately study the uncertainties in the cross-sections by varying one of these scales while keeping the other fixed at Q . In the left (right) panel, we present the renormalization (factorization) scale uncertainties in the invariant mass distribution up to NNLO+NNLL. In the case of resummation, the large partonic threshold logarithms are resummed to all orders in the perturbation series that is expanded in $a_s(\mu_R)$, and hence the uncertainties due to μ_R are expected to be smaller than those in the fixed order ones for a given μ_F , as can be seen from the Fig. [3]. However, the scale μ_F enters both the PDFs that are extracted at a fixed order as well as the parton coefficient functions, and hence the factorization scale uncertainty does not decrease as a result of resummation, as is evident from the right panel of Fig. [3]. Such a behaviour has already been reported in the literature [59, 60, 98–109].

In the context of scale uncertainties, we further study them by changing the choice of the central scale from Q to $Q/2$ and present the results for the invariant mass distribution in Tab. 1 for different Q values. We notice that the scale uncertainties for the central choice $\mu_R = \mu_F = Q/2$ at NNLO(NNLO+NNLL) are larger than those for the case of central choice $\mu_R = \mu_F = Q$. This behaviour is observed for the FO results as well as the resummed predictions, for all the Q values.

Further, in order to study the rate of convergence of the perturbative coefficient functions both in the fixed order as well as in the resummed predictions, it is useful to fix the PDF sets and study the K-factors like $K_{i,i-1}$, $R_{i,i-1}$ and $L_{i,i-1}$ (defined before), which are quite informative. Here, we chose the NNLO PDF sets and present the results up to NNLO+NNLL level in the Fig. [4]. Consequently, the same a_s is used at all orders. In the top left panel, we present the fixed order K-factors, K_{ij} . For a converging perturbation

Q(GeV)	Central scale = Q		Central scale = Q/2	
	NNLO	NNLO+NNLL	NNLO	NNLO+NNLL
165	0.74	1.74	0.99	2.14
565	2.25	2.02	2.50	2.23
1365	4.29	2.99	4.49	3.28
1765	5.22	3.43	5.48	3.72

Table 1. The 7-point scale uncertainty μ (in %) for the different central scale choices at different Q values.

series, the factor $K_{i,i-1}$ is supposed to be closer to unity with increasing i . While the K_{10} has the usual NLO K-factor information and is as large as 73%, from the K_{21} we see that the NNLO corrections could contribute an additional 40% of NLO results. Moreover, the K_{21} , is found to increase slowly with Q . Similar results are presented but for L_{ij} in the top right panel of Fig. [4]. By definition, these ratios will estimate the contribution of higher-order resummed results over and above at least the LO+LL level. Also, the term in the denominator already captures the contribution of large logarithms to a given accuracy, to all orders in the perturbation theory. Hence, these L_{ij} ratios are supposed to be smaller than the corresponding fixed order K-factors K_{ij} . In the bottom left panel of Fig. [4], we present the resummed K-factors R_{i0} to estimate the size of the resummed results above the LO predictions. We notice that the difference ($R_{20} - R_{10}$) is less than ($R_{10} - R_{00}$) for the whole invariant mass region considered here. Finally, in the bottom right panel of Fig. [4], we plot R_{ii} and notice that the contribution from the resummed corrections for any given i is smooth but slowly increases with Q . From R_{22} , we find that the size of higher logarithmic terms beyond NNLO is still large and are found to be around 6.2% of NNLO for $Q = 2500$ GeV. Apart from the theoretical uncertainties due to the unphysical scales in the calculation, there will also be uncertainties due to the non-perturbative PDFs. Here, using the LHAPDF routines, we estimate the intrinsic PDF uncertainties both in the fixed order NNLO results as well as the resummed NNLO+NNLL predictions for the invariant mass distribution, and present the same for different Q values in Tab. [2]. The PDFs are well constrained in the low x -region (where x is the Bjorken variable) compared to the high x -region, consequently the PDF uncertainties will increase with Q . These uncertainties are found to be about 1.52% at $Q = 165$ GeV and increase to 2.78% around 2000 GeV.

Q (GeV)	165	1365	1965
sym err (NNLO) %	1.52	2.33	2.80
sym err (NNLO+NNLL) %	1.52	2.32	2.78

Table 2. Intrinsic PDF error of NNPDF30_nnlo_as_01180_nf4 PDFs.

Finally, we study the total cross-section for the production of W -boson pairs at the LHC by integrating the invariant mass distribution from $Q = 2m_w$ to \sqrt{S} . For LHC energies, the total production cross-sections for the process under consideration are quite

large. Specially they are larger than those for the Z -boson pair production process due to the underlying parton fluxes, the corresponding couplings of the quarks to the gauge bosons and more importantly due to the additional s -channel contributions that are present in the case of W -boson pair production but are absent in the Z -boson pair production process.

\sqrt{S} (TeV)	7.0 TeV	13.0 TeV	13.6 TeV	14.0 TeV	100.0 TeV
LO	31.116 ^{+1.13%} _{-1.69%}	71.825 ^{+4.13%} _{-4.86%}	76.086 ^{+4.35%} _{-5.08%}	78.941 ^{+4.49%} _{-5.23%}	747.343 ^{+13.82%} _{-13.96%}
NLO	42.309 ^{+2.45%} _{-2.02%}	100.357 ^{+2.47%} _{-2.04%}	106.518 ^{+2.48%} _{-2.04%}	110.667 ^{+2.48%} _{-2.05%}	1130.054 ^{+3.84%} _{-5.63%}
NNLO _{$q\bar{q}$}	46.286 ^{+1.37%} _{-1.36%}	110.487 ^{+1.35%} _{-1.34%}	117.151 ^{+1.35%} _{-1.33%}	122.008 ^{+1.40%} _{-1.34%}	1248.098 ^{+1.69%} _{-1.81%}
NNLO	47.137 ^{+1.81%} _{-1.63%}	113.523 ^{+1.91%} _{-1.75%}	120.459 ^{+1.93%} _{-1.76%}	125.500 ^{+1.98%} _{-1.77%}	1323.434 ^{+2.84%} _{-2.47%}
LO+LL	34.710 ^{+1.44%} _{-2.02%}	79.387 ^{+4.43%} _{-5.16%}	84.055 ^{+4.65%} _{-5.39%}	87.183 ^{+4.79%} _{-5.53%}	814.504 ^{+14.12%} _{-14.20%}
NLO+NLL	43.766 ^{+3.13%} _{-3.18%}	103.464 ^{+3.81%} _{-4.14%}	109.794 ^{+3.86%} _{-4.21%}	114.057 ^{+3.90%} _{-4.26%}	1158.204 ^{+6.38%} _{-7.80%}
NNLO _{$q\bar{q}$} + NNLL	46.684 ^{+1.20%} _{-1.21%}	111.341 ^{+1.19%} _{-1.48%}	118.059 ^{+1.19%} _{-1.51%}	122.947 ^{+1.24%} _{-1.52%}	1255.799 ^{+1.76%} _{-2.72%}
NNLO+NNLL	47.536 ^{+1.58%} _{-1.45%}	114.378 ^{+1.75%} _{-1.58%}	121.367 ^{+1.77%} _{-1.60%}	126.439 ^{+1.82%} _{-1.61%}	1331.135 ^{+2.72%} _{-3.28%}

Table 3. Inclusive cross section (in pb) for W^+W^- boson pair production for different center of mass energies of the incoming protons, along with the corresponding 7-point scale uncertainties.

These production cross-sections have been given in the Tab. [3] up to NNLO+NNLL accuracy, along with the seven-point scale uncertainties, for different centre of mass energies of the incoming protons. For a given centre of mass energy, the cross-sections increase while the scale uncertainties are expected to decrease as we go from LO to NNLO. However, here it is observed that the scale uncertainties increase from NLO to NNLO. This is due to the presence of the gluon fusion channel that opens up from the second order in perturbation theory, and hence new contributions will add to the renormalization scale uncertainties. The gluon fluxes for the LHC energies near the $2m_w$ region are quite large, and this gluon fusion channel contributes about 4.2% of LO for 13.6 TeV LHC energy. The NLO corrections for the gluon fusion channel, in the massless quark limit, are about 60% of its LO for 13 TeV LHC energy [110]. To systematically quantify the uncertainties in the perturbation theory, we define the second-order cross-section without this gluon fusion channel and call it NNLO _{$q\bar{q}$} . The scale uncertainties in the total production cross-sections, LO, NLO, and NNLO _{$q\bar{q}$} are found to systematically decrease from 5.1% to 1.4% for 13.6 TeV LHC as can be seen from the Tab. [3].

A similar behaviour can be noticed for the resummed results as well, where the scale uncertainties decrease from 5.4% to 1.5%, as we go from LO+LL to NNLO+NNLL. However, the resummed results in general have larger scale uncertainties compared to those in the corresponding fixed-order results. This is simply because of the definition of total production cross-section, somewhere the dominant contribution to the cross-section comes from the lower invariant mass region, when integrated out from $Q_{\min} = 2m_w$ to \sqrt{S} . In the lower Q -region, both the regular terms as well as other subprocesses like qg contribute, substantially leading to the reduction of the scale uncertainties in the fixed order results. However, with increasing Q_{\min} in the total production cross-section, the threshold logarithms start dominating the cross-sections and tend to reduce the scale uncertainties in the NNLO+NNLL results, as evident from Fig. [2].

4 Summary

In our article, we have presented threshold resummation for the production of a pair of on-shell W -bosons. We have performed the resummation at NNLO+NNLL accuracy, and give our results up to $Q = 2500$ GeV. On the top of the available NNLO results, the NNLL resummed results are found to contribute an additional 1% of LO at $Q = 165$ GeV and rise to as large as 13% at $Q = 2500$ GeV. We have further compared and contrasted these NNLO+NNLL resummed results with those at NLO+NNLL accuracy, and find that the former have less scale uncertainties throughout the invariant mass region considered here.

In addition, we have investigated the effect of the intrinsic PDF uncertainty. While the PDF uncertainty at NNLO is 2.80% at $Q = 1965$ GeV, the corresponding one at NNLO+NNLL is about 2.78%. In contrast, for the invariant mass distribution, 7-point scale uncertainties decrease from 5.7% at NNLO to 3.6% at NNLO+NNLL, at the same value of Q . This highlights the importance of our resummation results. We have also studied the convergence of the perturbative series by evaluating the fixed order and resummed results using the same NNLO order PDFs. Moreover, we investigate the behaviour of the seven point scale uncertainties by changing the choice of central scale from Q to $Q/2$, and observe that the choice of central scale Q has smaller uncertainties both for fixed-order as well as resummed results. The present results at NNLO+NNLL are the most precise results available to-date in the perturbative QCD for the invariant mass distribution of W -boson pair production process and are expected to augment the precision studies at the current LHC as well as at the future hadron colliders.

Acknowledgements

P.B. acknowledges A. Papa for useful discussion. The research work of M.C.K. is supported by SERB Core Research Grant (CRG) under the project CRG/2021/005270. The work of P.B. is supported by the INFN/QFT@COLLIDERS project (Italy). We acknowledge National Supercomputing Mission (NSM) for providing computing resources of ‘PARAM Kamrupa’ at IIT Guwahati, which is implemented by C-DAC and supported by the Ministry of Electronics and Information Technology (MeitY) and Department of Science and Technology (DST), Government of India, where most of the computational work has been carried out. P.B. acknowledges the Department of Physics at the University of Calabria for providing computing resources.

A Resummation coefficients

The process-dependent g_0 coefficients defined in Eq. (2.18) are given as (defining $L_{qr} = \ln(Q^2/\mu_R^2)$, $L_{fr} = \ln(\mu_F^2/\mu_R^2)$),

$$g_{01} = 2\mathcal{A}_{(0,1)} + 2C_F \left\{ -3L_{fr} + L_{qr}^2 + \zeta_2 \right\}, \quad (\text{A.1})$$

$$\begin{aligned} g_{02} = & \mathcal{A}_{(1,1)} + 2\mathcal{A}_{(0,2)} + C_F n_f \left\{ -\frac{328}{21} + \frac{2}{3}L_{fr} + \frac{112}{27}L_{qr} - \frac{20}{9}L_{qr}^2 - \frac{10}{9}\zeta_2 + \frac{16}{3}L_{fr}\zeta_2 \right. \\ & \left. - \frac{4}{3}L_{qr}\zeta_2 + \frac{32}{3}\zeta_3 \right\} + C_F^2 \left\{ -3L_{fr} + 18L_{fr}^2 - 12L_{fr}L_{qr}^2 + 2L_{qr}^4 + 12L_{fr}\zeta_2 + 4L_{qr}^2\zeta_2 \right. \\ & \left. + 2\zeta_2^2 - 48L_{fr}\zeta_3 \right\} + C_F \left\{ +3\beta_0 L_{fr}^2 - \frac{2}{3}\beta_0 L_{qr}^3 - 12L_{fr}\mathcal{A}_{(0,1)} + 4L_{qr}^2\mathcal{A}_{(0,1)} - 6b\beta_0\zeta_2 \right. \\ & \left. - 2\beta_0 L_{qr}\zeta_2 + 4\mathcal{A}_{(0,1)}\zeta_2 + \frac{32}{3}\beta_0\zeta_3 \right\} + C_F C_A \left\{ +\frac{2428}{81} - \frac{17}{3}L_{fr} - \frac{808}{27}L_{qr} + \frac{134}{9}L_{qr}^2 \right. \\ & \left. + \frac{67}{9}\zeta_2 - \frac{88}{3}L_{fr}\zeta_2 + \frac{22}{3}L_{qr}\zeta_2 - 4L_{qr}^2\zeta_2 - 12\zeta_2^2 - \frac{176}{3}\zeta_3 + 24L_{fr}\zeta_3 + 28L_{qr}\zeta_3 \right\} \end{aligned} \quad (\text{A.2})$$

Here, we define

$$\mathcal{A}_{(m,n)} = \frac{\mathcal{M}_{(m,n)}^{\text{fin}}}{\mathcal{M}_{(0,0)}} \quad (\text{A.3})$$

where,

$$\mathcal{M}_{(m,n)}^{\text{fin}} \equiv \langle \mathcal{M}_m | \mathcal{M}_n \rangle \quad (\text{A.4})$$

and $|\mathcal{M}_n\rangle$ represents the UV-renormalized, IR-finite virtual amplitude at the n-th order in a_s , as given in Eq. (C3) of Ref. [88]. The one loop virtual contribution for W^+W^- pair production (u -type) is ,

$$\mathcal{M}_{0,1} = \frac{\alpha_s}{4\pi} B_f N C_f (c_{tt}\mathcal{F}_1 - c_{ts}\mathcal{J}_1 + c_{ss}\mathcal{K}_1) \quad (\text{A.5})$$

$$\mathcal{F}_1 = \mathcal{I}_1\mathcal{F}_0 + \mathcal{F}_1^{\text{fin}}, \quad \mathcal{J}_1 = \mathcal{I}_1\mathcal{J}_0 + \mathcal{J}_1^{\text{fin}}, \quad \mathcal{K}_1 = \mathcal{I}_1\mathcal{K}_0 + \mathcal{K}_1^{\text{fin}} \quad (\text{A.6})$$

where,

$$\mathcal{I}_1 = -\frac{e^{\epsilon\gamma_E}}{\Gamma(1-\epsilon)} \left(\frac{\mu^2}{s} \right)^\epsilon \left\{ \frac{1}{\epsilon^2} + \frac{1}{\epsilon} \left(i\pi - \frac{3}{2} \right) \right\} C_F. \quad (\text{A.7})$$

$$\mathcal{F}_1^{\text{fin}} = \frac{1}{((-1+x)^5 x (1+x)y^2)} [4(-8x^4 y(3+2y^2)\zeta_2 + y(18+y^2(4-3\zeta_2) - 12\zeta_2$$

$$\begin{aligned}
& -4y(-4 + 3\zeta_2) + x^8y(-18 + 4\zeta_2 + 4y(-4 + 3\zeta_2) + y^2(-4 + 3\zeta_2)) + x^7(18 \\
& + y^2(50 - 31\zeta_2) + y^4(4 - 3\zeta_2) - 4\zeta_2 - 4y^3(-4 + 3\zeta_2) - 8y(-9 + 4\zeta_2)) + 2x^6 \\
& (-36 + 8\zeta_2 + 6y^2(-4 + 3\zeta_2) + 4y(-13 + 5\zeta_2) + y^4(-8 + 6\zeta_2) + y^3(-10 + 9\zeta_2)) \\
& - 2x^2(-36 + 2y^2(-12 + \zeta_2) + 8\zeta_2 + y^4(-8 + 6\zeta_2) + 4y(-13 + 7\zeta_2) + y^3(-10 \\
& + 9\zeta_2)) + x^5(90 + y^3(8 - 28\zeta_2) - 32y(-2 + \zeta_2) - 20\zeta_2 - 5y^4(-4 + 3\zeta_2) + 5y^2 \\
& (2 + 9\zeta_2)) + x^3(-90 + 32y(-2 + \zeta_2) + 20\zeta_2 - 4y^3(2 + \zeta_2) + 5y^4(-4 + 3\zeta_2) + \\
& y^2(-10 + 11\zeta_2)) + x(-18 + 4\zeta_2 + 4y^3(-4 + 3\zeta_2) + y^4(-4 + 3\zeta_2) + 8y(-9 + 4\zeta_2) \\
& + y^2(-50 + 39\zeta_2))) + i(2\pi(y(24 + 20y + 15y^2 + 3y^3) + x^2y(24 + 20y + 15y^2 + \\
& 3y^3) + x(-24 + 5y^2 + 13y^3 - 3y^4 - 3y^5))) + [\log(x) - 2\log(1 + x)] \left\{ \frac{1}{(-1 + x)^4xy^2} \right. \\
& 8(3y + 3x^6y - x(3 + 6y + 7y^2) - x^5(3 + 6y + 7y^2) + x^2(12 + 19y + 2y^3) + x^4(12 \\
& + 19y + 2y^3) + 2x^3(-9 - 10y - 5y^2 + 4y^3)) + i\left(\frac{1}{xy^2}16\pi(y + x^2y - x(2 + y^2))\right) \left. \right\} + \\
& \log(y) \left\{ -\frac{1}{xy^2(1 + y)}8(y(3 - y + 2i\pi(1 + y)) + x^2y(3 - y + 2i\pi(1 + y)) - x(3 \right. \\
& - 3y + y^2 - y^3 + 2i\pi(2 + 2y + y^2 + y^3))) \left. \right\} + \left[\log(1 + y) - \frac{1}{4i\pi}\log(y)^2 + \frac{1}{2i\pi} \times \right. \\
& \log(1 + y)^2 + \frac{1}{i\pi}Li_2\left(\frac{1}{1 + y}\right) + \frac{1}{2i\pi}\log(x)\log(y) - \frac{1}{i\pi}\log(1 + x)\log(y) \left. \right] \left(\frac{32i\pi}{xy^2} \times \right. \\
& (y + x^2y - x(2 + y^2)) \left. \right) + [\log(x)^2 + 4Li_2(-x)] \left\{ \frac{-1}{(-1 + x)^5x(1 + x)y} (32(1 + \right. \\
& x^8 + x^2(2 - 4y) + x^6(2 - 4y) - xy - x^7y + x^3y(-7 + 4y) + x^5y(-7 + 4y) + \\
& x^4(6 + 4y^2)) \left. \right\} \tag{A.8}
\end{aligned}$$

$$\begin{aligned}
\mathcal{J}_1^{fin} = & \frac{-1}{3(-1 + x)^3x^2(1 + x)y(1 + y)^2} \left[m_w^2(8\pi^2x^4y(1 + y)^2(4 + 3y) + x^8y(6i\pi(20 + 31y \right. \\
& + 18y^2 + 3y^3) - (1 + y)(5\pi^2(4 + 5y + y^2) + 6(4(-9 + \zeta_2) + 5y(-8 + \zeta_2) + y^2(\\
& - 8 + \zeta_2)))) + y(-6i\pi(20 + 31y + 18y^2 + 3y^3) + (1 + y)(5\pi^2(4 + 5y + y^2) + 6 \times \\
& (4(-9 + \zeta_2) + 5y(-8 + \zeta_2) + y^2(-8 + \zeta_2)))) + x^3(6i\pi(-144 - 227y - 156y^2 - \\
& 60y^3 - 8y^4 + 3y^5) - (1 + y)(\pi^2(-96 - 79y - 29y^2 - 41y^3 + 5y^4) + 6(272 + y(\\
& 286 - 35\zeta_2) + y^3(44 - 5\zeta_2) - 9y^2(-10 + \zeta_2) + y^4(-8 + \zeta_2) - 32\zeta_2))) + x^5(6i\pi \times \\
& (144 + 227y + 156y^2 + 60y^3 + 8y^4 - 3y^5) + (1 + y)(\pi^2(-96 - 87y + 11y^2 + 7y^3 \\
& + 5y^4) + 6(272 + y(286 - 35\zeta_2) + y^3(44 - 5\zeta_2) - 9y^2(-10 + \zeta_2) + y^4(-8 + \zeta_2) \\
& - 32\zeta_2))) - 2x^2(6i\pi(-9 - 49y - 61y^2 - 24y^3 + 4y^4 + 3y^5) - (1 + y)(\pi^2(-6 - \\
& 57y - 56y^2 + 5y^4) + 6(17 + y^3 + y(79 - 9\zeta_2) + y^2(67 - 8\zeta_2) + y^4(-8 + \zeta_2) - \\
& 2\zeta_2))) + 2x^6(6i\pi(-9 - 49y - 61y^2 - 24y^3 + 4y^4 + 3y^5) - (1 + y)(\pi^2(-6 - 17y \\
& - 12y^2 + 4y^3 + 5y^4) + 6(17 + y^3 + y(79 - 9\zeta_2) + y^2(67 - 8\zeta_2) + y^4(-8 + \zeta_2) \\
& - 2\zeta_2))) + x^7(-6i\pi(36 + 37y + 12y^2 + 12y^3 + 12y^4 + 3y^5) + (1 + y)(\pi^2(24 + y
\end{aligned}$$

$$\begin{aligned}
& -13y^2 + 15y^3 + 5y^4) + 6(-68 + 3y^3(-8 + \zeta_2) + y^4(-8 + \zeta_2) - y^2(-6 + \zeta_2) + \\
& 8\zeta_2 + y(-38 + 5\zeta_2))) + x(6i\pi(36 + 37y + 12y^2 + 12y^3 + 12y^4 + 3y^5) - (1 + y) \\
& (\pi^2(24 + 9y - 5y^2 + 15y^3 + 5y^4) + 6(-68 + 3y^3(-8 + \zeta_2) + y^4(-8 + \zeta_2) - y^2(- \\
& -6 + \zeta_2) + 8\zeta_2 + y(-38 + 5\zeta_2)))) + \left[\log(x) - 2\log(1 + x) \right] \left\{ \frac{-1}{(-1 + x)^2 xy} \right. \\
& 4m_w^2(3(2 + y) + 3x^4(2 + y) + x(3 + 10y - y^2) + x^3(3 + 10y - y^2) - 2x^2(9 + 5y \\
& + 7y^2) + 2i\pi(-1 + x)^2(4 + y + x^2(4 + y) + x(10 + 4y + y^2))) \left. \right\} + \log(y) \left\{ \right. \\
& \frac{1}{(x^2 y(1 + y)^2)} 4m_w^2(-2y(2 + y) - 2x^4 y(2 + y) + x(6 - 9y - 4y^2 + 3y^3 + 2i\pi(1 \\
& + y)^2(4 + y)) + x^3(6 - 9y - 4y^2 + 3y^3 + 2i\pi(1 + y)^2(4 + y)) + x^2(15 - 2y \\
& + 2y^2 + 6y^3 - y^4 + 2i\pi(1 + y)^2(10 + 4y + y^2))) \left. \right\} + \left[\log(1 + y) - \frac{1}{4i\pi} \log(y)^2 \right. \\
& + \frac{1}{2i\pi} \log(1 + y)^2 + \frac{1}{i\pi} Li_2\left(\frac{1}{1 + y}\right) + \frac{1}{2i\pi} \log(x) \log(y) - \frac{1}{i\pi} \log(1 + x) \log(y) \left. \right] \\
& \left\{ \frac{-16im_w^2 \pi}{xy} (4 + y + x^2(4 + y) + x(10 + 4y + y^2)) \right\} + \left[\log(x)^2 + 4Li_2(-x) \right] \left\{ \right. \\
& \frac{4m_w^2}{(-1 + x)^3 x(1 + x)} (1 + x^6 + x^2(1 - 6y) + x^4(1 - 6y) + x(10 + y) + x^5(10 + y) \\
& \left. - 2x^3(4 + 3y)) \right\} \tag{A.9}
\end{aligned}$$

$$\begin{aligned}
\mathcal{K}_1^{fin} = & \frac{1}{x^3} 2m_w^4 \left(4 + y + x^6(4 + y) + x^2(-4 + 11y) + x^4(-4 + 11y) - x(-7 + y^2) - \right. \\
& \left. x^5(-7 + y^2) - 2x^3(13 + 5y^2) \right) (-4 + 3\zeta_2) \tag{A.10}
\end{aligned}$$

Similar to Eq. 2.11 we can write the amplitudes for the d -type quark process.

$$\mathcal{F}_1^d(x, z) = \mathcal{F}_1^u(x, y), \quad \mathcal{J}_1^d(x, z) = -\mathcal{J}_1^u(x, y), \quad \mathcal{K}_1^d(x, z) = \mathcal{K}_1^u(x, y). \tag{A.11}$$

The process-independent universal resum exponent defined in Eq. (2.17) which are used for DY-type processes are given as,

$$g_1 = \left[\frac{A_1}{\beta_0} \left\{ 2 - 2 \ln(1 - \omega) + 2 \ln(1 - \omega) \omega^{-1} \right\} \right], \tag{A.12}$$

$$\begin{aligned}
g_2 = & \left[\frac{D_1}{\beta_0} \left\{ \frac{1}{2} \ln(1 - \omega) \right\} + \frac{A_2}{\beta_0^2} \left\{ -\ln(1 - \omega) - \omega \right\} + \frac{A_1}{\beta_0} \left\{ \left(\ln(1 - \omega) + \frac{1}{2} \ln(1 - \omega)^2 \right. \right. \right. \\
& \left. \left. + \omega \right) \left(\frac{\beta_1}{\beta_0^2} \right) + \left(\omega \right) L_{fr} + \left(\ln(1 - \omega) \right) L_{qr} \right\} \right], \tag{A.13}
\end{aligned}$$

$$\begin{aligned}
g_3 = & \left[\frac{A_3}{\beta_0^2} \left\{ -\frac{\omega}{(1 - \omega)} + \omega \right\} + \frac{A_2}{\beta_0} \left\{ \left(2 \frac{\omega}{(1 - \omega)} \right) L_{qr} + \left(3 \frac{\omega}{(1 - \omega)} + 2 \frac{\ln(1 - \omega)}{(1 - \omega)} \right. \right. \right. \\
& \left. \left. - \omega \right) \left(\frac{\beta_1}{\beta_0^2} \right) + \left(-2 \omega \right) L_{fr} \right\} + A_1 \left\{ -4 \zeta_2 \frac{\omega}{(1 - \omega)} + \left(-\frac{\ln(1 - \omega)^2}{(1 - \omega)} - \frac{\omega}{(1 - \omega)} \right) \right.
\end{aligned}$$

$$\begin{aligned}
& -2 \frac{\ln(1-\omega)}{(1-\omega)} + 2 \ln(1-\omega) + \omega \left) \left(\frac{\beta_1}{\beta_0^2} \right)^2 + \left(-\frac{\omega}{(1-\omega)} \right) L_{qr}^2 + \left(-\frac{\omega}{(1-\omega)} \right. \\
& -2 \ln(1-\omega) - \omega \left) \left(\frac{\beta_2}{\beta_0^3} \right) + \left(\left(-2 \frac{\omega}{(1-\omega)} - 2 \frac{\ln(1-\omega)}{(1-\omega)} \right) \left(\frac{\beta_1}{\beta_0^2} \right) \right) L_{qr} \\
& + \left(\omega \right) L_{fr}^2 \left. \right\} + \frac{D_2}{\beta_0} \left\{ \frac{\omega}{(1-\omega)} \right\} + D_1 \left\{ \left(-\frac{\omega}{(1-\omega)} \right) L_{qr} + \left(-\frac{\omega}{(1-\omega)} \right. \right. \\
& \left. \left. - \frac{\ln(1-\omega)}{(1-\omega)} \right) \left(\frac{\beta_1}{\beta_0^2} \right) \right\} \left. \right\}, \tag{A.14}
\end{aligned}$$

Here A_i are the universal cusp anomalous dimensions, D_i are the threshold non-cusp anomalous dimensions, and $\omega = 2a_s\beta_0 \ln \bar{N}$. Note that all the perturbative quantities are expanded in powers of a_s . The cusp anomalous dimensions A_i are given as (recently four-loops results are available can be found in Ref. [111–113]),

$$A_1 = C_F \left\{ 4 \right\}, \tag{A.15}$$

$$A_2 = C_F \left\{ n_f \left(-\frac{40}{9} \right) + C_A \left(\frac{268}{9} - 8\zeta_2 \right) \right\}, \tag{A.16}$$

$$\begin{aligned}
A_3 = C_F \left\{ n_f^2 \left(-\frac{16}{27} \right) + C_F n_f \left(-\frac{110}{3} + 32\zeta_3 \right) + C_A n_f \left(-\frac{836}{27} - \frac{112}{3}\zeta_3 + \frac{160}{9}\zeta_2 \right) \right. \\
\left. + C_A^2 \left(\frac{490}{3} + \frac{88}{3}\zeta_3 - \frac{1072}{9}\zeta_2 + \frac{176}{5}\zeta_2^2 \right) \right\}, \tag{A.17}
\end{aligned}$$

The coefficients D_i are given as,

$$D_1 = C_F \left\{ 0 \right\}, \tag{A.18}$$

$$D_2 = C_F \left\{ n_f \left(\frac{224}{27} - \frac{32}{3}\zeta_2 \right) + C_A \left(-\frac{1616}{27} + 56\zeta_3 + \frac{176}{3}\zeta_2 \right) \right\}, \tag{A.19}$$

Here,

$$C_A = N, \quad C_F = \frac{N^2 - 1}{2N}, \tag{A.20}$$

$$\beta_0 = \frac{11}{3}C_A - \frac{2}{3}n_f, \tag{A.21}$$

$$\beta_1 = \frac{34}{3}C_A^2 - \frac{10}{3}n_f C_A - 2n_f C_F, \tag{A.22}$$

$$\beta_2 = \frac{2857}{54}C_A^3 - \frac{1415}{54}n_f C_A^2 - \frac{205}{18}n_f C_F C_A + n_f C_F^2 + \frac{79}{54}n_f^2 C_A + \frac{11}{9}n_f^2 C_F. \tag{A.23}$$

References

- [1] ATLAS collaboration, G. Aad et al., *Observation of a new particle in the search for the Standard Model Higgs boson with the ATLAS detector at the LHC*, *Phys. Lett. B* **716** (2012) 1 [1207.7214].
- [2] CMS collaboration, S. Chatrchyan et al., *Observation of a New Boson at a Mass of 125 GeV with the CMS Experiment at the LHC*, *Phys. Lett. B* **716** (2012) 30 [1207.7235].

- [3] CMS collaboration, A. Hayrapetyan et al., *Search for a resonance decaying to a W boson and a photon in proton-proton collisions at $\sqrt{s} = 13$ TeV using leptonic W boson decays*, *JHEP* **09** (2024) 186 [[2406.05737](#)].
- [4] CMS collaboration, A. Hayrapetyan et al., *Search for new physics in high-mass diphoton events from proton-proton collisions at $\sqrt{s} = 13$ TeV*, *JHEP* **08** (2024) 215 [[2405.09320](#)].
- [5] ATLAS collaboration, G. Aad et al., *Search for Nearly Mass-Degenerate Higgsinos Using Low-Momentum Mildly Displaced Tracks in pp Collisions at $s=13$ TeV with the ATLAS Detector*, *Phys. Rev. Lett.* **132** (2024) 221801 [[2401.14046](#)].
- [6] CMS collaboration, V. Chekhovsky et al., *High-precision measurement of the W boson mass with the CMS experiment at the LHC*, [2412.13872](#).
- [7] S. Heinemeyer, W. Hollik, G. Weiglein and L. Zeune, *Implications of LHC search results on the W boson mass prediction in the MSSM*, *JHEP* **12** (2013) 084 [[1311.1663](#)].
- [8] CMS collaboration, A. Hayrapetyan et al., *Measurement of inclusive and differential cross sections for W^+W^- production in proton-proton collisions at $\sqrt{s} = 13.6$ TeV*, *Phys. Lett. B* **861** (2025) 139231 [[2406.05101](#)].
- [9] ATLAS collaboration, G. Aad et al., *Measurements of W^+W^- production in decay topologies inspired by searches for electroweak supersymmetry*, *Eur. Phys. J. C* **83** (2023) 718 [[2206.15231](#)].
- [10] R. W. Brown and K. O. Mikaelian, *W^+W^- and Z^0Z^0 Pair Production in e^+e^- , pp , $p\bar{p}$ Colliding Beams*, *Phys. Rev. D* **19** (1979) 922.
- [11] J. Ohnemus, *An Order α^-s calculation of hadronic W^-W^+ production*, *Phys. Rev. D* **44** (1991) 1403.
- [12] S. Frixione, *A Next-to-leading order calculation of the cross-section for the production of W^+W^- pairs in hadronic collisions*, *Nucl. Phys. B* **410** (1993) 280.
- [13] L. J. Dixon, Z. Kunszt and A. Signer, *Helicity amplitudes for $O(\alpha_s)$ production of W^+W^- , $W^\pm Z$, ZZ , $W^\pm\gamma$, or $Z\gamma$ pairs at hadron colliders*, *Nucl. Phys. B* **531** (1998) 3 [[hep-ph/9803250](#)].
- [14] J. M. Campbell and R. K. Ellis, *An Update on vector boson pair production at hadron colliders*, *Phys. Rev. D* **60** (1999) 113006 [[hep-ph/9905386](#)].
- [15] L. J. Dixon, Z. Kunszt and A. Signer, *Vector boson pair production in hadronic collisions at order α_s : Lepton correlations and anomalous couplings*, *Phys. Rev. D* **60** (1999) 114037 [[hep-ph/9907305](#)].
- [16] S. Dittmaier, S. Kallweit and P. Uwer, *NLO QCD corrections to WW +jet production at hadron colliders*, *Phys. Rev. Lett.* **100** (2008) 062003 [[0710.1577](#)].
- [17] J. M. Campbell, R. K. Ellis and G. Zanderighi, *Next-to-leading order predictions for $WW + 1$ jet distributions at the LHC*, *JHEP* **12** (2007) 056 [[0710.1832](#)].
- [18] S. Dittmaier, S. Kallweit and P. Uwer, *NLO QCD corrections to $pp/ppbar \rightarrow WW$ +jet+ X including leptonic W -boson decays*, *Nucl. Phys. B* **826** (2010) 18 [[0908.4124](#)].
- [19] K. Hamilton, T. Melia, P. F. Monni, E. Re and G. Zanderighi, *Merging WW and WW +jet with MINLO*, *JHEP* **09** (2016) 057 [[1606.07062](#)].
- [20] T. Melia, K. Melnikov, R. Rontsch and G. Zanderighi, *NLO QCD corrections for W^+W^-*

- pair production in association with two jets at hadron colliders, *Phys. Rev. D* **83** (2011) 114043 [[1104.2327](#)].
- [21] N. Greiner, G. Heinrich, P. Mastrolia, G. Ossola, T. Reiter and F. Tramontano, *NLO QCD corrections to the production of $W^+ W^-$ plus two jets at the LHC*, *Phys. Lett. B* **713** (2012) 277 [[1202.6004](#)].
- [22] F. Febres Cordero, P. Hofmann and H. Ita, *$W^+W^- + 3$ -jet production at the Large Hadron Collider in next-to-leading-order QCD*, *Phys. Rev. D* **95** (2017) 034006 [[1512.07591](#)].
- [23] M. Grazzini, *Soft-gluon effects in WW production at hadron colliders*, *JHEP* **01** (2006) 095 [[hep-ph/0510337](#)].
- [24] P. Meade, H. Ramani and M. Zeng, *Transverse momentum resummation effects in W^+W^- measurements*, *Phys. Rev. D* **90** (2014) 114006 [[1407.4481](#)].
- [25] Y. Wang, C. S. Li, Z. L. Liu, D. Y. Shao and H. T. Li, *Transverse-Momentum Resummation for Gauge Boson Pair Production at the Hadron Collider*, *Phys. Rev. D* **88** (2013) 114017 [[1307.7520](#)].
- [26] P. Jaiswal and T. Okui, *Explanation of the WW excess at the LHC by jet-veto resummation*, *Phys. Rev. D* **90** (2014) 073009 [[1407.4537](#)].
- [27] A. Bierweiler, T. Kasprzik, J. H. Kühn and S. Uccirati, *Electroweak corrections to W -boson pair production at the LHC*, *JHEP* **11** (2012) 093 [[1208.3147](#)].
- [28] J. Baglio, L. D. Ninh and M. M. Weber, *Massive gauge boson pair production at the LHC: a next-to-leading order story*, *Phys. Rev. D* **88** (2013) 113005 [[1307.4331](#)].
- [29] M. Billoni, S. Dittmaier, B. Jäger and C. Speckner, *Next-to-leading order electroweak corrections to $pp \rightarrow W^+W^- \rightarrow 4$ leptons at the LHC in double-pole approximation*, *JHEP* **12** (2013) 043 [[1310.1564](#)].
- [30] J. Baglio, S. Dawson and I. M. Lewis, *An NLO QCD effective field theory analysis of W^+W^- production at the LHC including fermionic operators*, *Phys. Rev. D* **96** (2017) 073003 [[1708.03332](#)].
- [31] J. Baglio, S. Dawson and I. M. Lewis, *NLO effects in EFT fits to W^+W^- production at the LHC*, *Phys. Rev. D* **99** (2019) 035029 [[1812.00214](#)].
- [32] A. Denner and G. Pelliccioli, *Polarized electroweak bosons in W^+W^- production at the LHC including NLO QCD effects*, *JHEP* **09** (2020) 164 [[2006.14867](#)].
- [33] R. Poncelet and A. Popescu, *NNLO QCD study of polarised W^+W^- production at the LHC*, *JHEP* **07** (2021) 023 [[2102.13583](#)].
- [34] T. Gehrmann, M. Grazzini, S. Kallweit, P. Maierhöfer, A. von Manteuffel, S. Pozzorini et al., *W^+W^- Production at Hadron Colliders in Next to Next to Leading Order QCD*, *Phys. Rev. Lett.* **113** (2014) 212001 [[1408.5243](#)].
- [35] F. Caola, J. M. Henn, K. Melnikov, A. V. Smirnov and V. A. Smirnov, *Two-loop helicity amplitudes for the production of two off-shell electroweak bosons in quark-antiquark collisions*, *JHEP* **11** (2014) 041 [[1408.6409](#)].
- [36] T. Gehrmann, A. von Manteuffel and L. Tancredi, *The two-loop helicity amplitudes for $q\bar{q}' \rightarrow V_1V_2 \rightarrow 4$ leptons*, *JHEP* **09** (2015) 128 [[1503.04812](#)].
- [37] M. Grazzini, S. Kallweit, S. Pozzorini, D. Rathlev and M. Wiesemann, *W^+W^- production*

- at the LHC: fiducial cross sections and distributions in NNLO QCD, *JHEP* **08** (2016) 140 [1605.02716].
- [38] M. Grazzini, S. Kallweit, J. M. Lindert, S. Pozzorini and M. Wiesemann, *NNLO QCD + NLO EW with Matrix+OpenLoops: precise predictions for vector-boson pair production*, *JHEP* **02** (2020) 087 [1912.00068].
- [39] W.-J. He, R.-Y. Zhang, L. Han, Y. Jiang, Z. Li, X.-F. Wang et al., *Two-loop planar master integrals for NNLO QCD corrections to W-pair production in quark-antiquark annihilation*, *JHEP* **12** (2024) 136 [2409.08879].
- [40] J. M. Campbell, R. K. Ellis and C. Williams, *Vector Boson Pair Production at the LHC*, *JHEP* **07** (2011) 018 [1105.0020].
- [41] E. W. N. Glover and J. J. van der Bij, *VECTOR BOSON PAIR PRODUCTION VIA GLUON FUSION*, *Phys. Lett. B* **219** (1989) 488.
- [42] T. Binoth, M. Ciccolini, N. Kauer and M. Kramer, *Gluon-induced WW background to Higgs boson searches at the LHC*, *JHEP* **03** (2005) 065 [hep-ph/0503094].
- [43] T. Binoth, M. Ciccolini, N. Kauer and M. Kramer, *Gluon-induced W-boson pair production at the LHC*, *JHEP* **12** (2006) 046 [hep-ph/0611170].
- [44] F. Caola, J. M. Henn, K. Melnikov, A. V. Smirnov and V. A. Smirnov, *Two-loop helicity amplitudes for the production of two off-shell electroweak bosons in gluon fusion*, *JHEP* **06** (2015) 129 [1503.08759].
- [45] A. von Manteuffel and L. Tancredi, *The two-loop helicity amplitudes for $gg \rightarrow V_1 V_2 \rightarrow 4$ leptons*, *JHEP* **06** (2015) 197 [1503.08835].
- [46] F. Caola, K. Melnikov, R. Röntsch and L. Tancredi, *QCD corrections to W^+W^- production through gluon fusion*, *Phys. Lett. B* **754** (2016) 275 [1511.08617].
- [47] M. Grazzini, S. Kallweit, D. Rathlev and M. Wiesemann, *Transverse-momentum resummation for vector-boson pair production at NNLL+NNLO*, *JHEP* **08** (2015) 154 [1507.02565].
- [48] S. Dawson, P. Jaiswal, Y. Li, H. Ramani and M. Zeng, *Resummation of jet veto logarithms at $N^3LL_a + NNLO$ for W^+W^- production at the LHC*, *Phys. Rev. D* **94** (2016) 114014 [1606.01034].
- [49] S. Dawson, I. M. Lewis and M. Zeng, *Threshold resummed and approximate next-to-next-to-leading order results for W^+W^- pair production at the LHC*, *Phys. Rev. D* **88** (2013) 054028 [1307.3249].
- [50] E. Re, M. Wiesemann and G. Zanderighi, *NNLOPS accurate predictions for W^+W^- production*, *JHEP* **12** (2018) 121 [1805.09857].
- [51] D. Lombardi, M. Wiesemann and G. Zanderighi, *W^+W^- production at NNLO+PS with MINNLO_{PS}*, *JHEP* **11** (2021) 230 [2103.12077].
- [52] A. Gavardi, M. A. Lim, S. Alioli and F. J. Tackmann, *NNLO+PS W^+W^- production using jet veto resummation at NNLL'*, *JHEP* **12** (2023) 069 [2308.11577].
- [53] CMS collaboration, A. M. Sirunyan et al., *Measurements of $pp \rightarrow ZZ$ production cross sections and constraints on anomalous triple gauge couplings at $\sqrt{s} = 13$ TeV*, *Eur. Phys. J. C* **81** (2021) 200 [2009.01186].

- [54] FCC collaboration, A. Abada et al., *FCC-hh: The Hadron Collider: Future Circular Collider Conceptual Design Report Volume 3*, *Eur. Phys. J. ST* **228** (2019) 755.
- [55] CDF collaboration, T. Affolder et al., *Measurement of $d(\sigma)/dM$ and Forward-Backward Charge Asymmetry for High Mass Drell-Yan e^+e^- Pairs from $p\bar{p}$ Collisions at $\sqrt{s} = 1.8$ TeV*, *Phys. Rev. Lett.* **87** (2001) 131802 [[hep-ex/0106047](#)].
- [56] CMS collaboration, S. Chatrchyan et al., *Measurement of the Drell-Yan Cross Section in pp Collisions at $\sqrt{s} = 7$ TeV*, *JHEP* **10** (2011) 007 [[1108.0566](#)].
- [57] ATLAS collaboration, G. Aad et al., *Measurement of the high-mass Drell-Yan differential cross-section in pp collisions at $\sqrt{s}=7$ TeV with the ATLAS detector*, *Phys. Lett. B* **725** (2013) 223 [[1305.4192](#)].
- [58] CMS collaboration, A. M. Sirunyan et al., *Measurement of the differential Drell-Yan cross section in proton-proton collisions at $\sqrt{s} = 13$ TeV*, *JHEP* **12** (2019) 059 [[1812.10529](#)].
- [59] G. Das, C. Dey, M. C. Kumar and K. Samanta, *Threshold enhanced cross sections for colorless productions*, *Phys. Rev. D* **107** (2023) 034038 [[2210.17534](#)].
- [60] P. Banerjee, C. Dey, M. C. Kumar and V. Pandey, *Threshold resummation for Z-boson pair production at NNLO+NNLL*, [2409.16375](#).
- [61] S. A. Larin, *Theoretical aspects of quantum field theory*, *Journal of Theoretical Physics* **27** (1993) 123.
- [62] S. Moch, J. A. M. Vermaseren and A. Vogt, *Three-loop results for quark and gluon form-factors*, *Phys. Lett. B* **625** (2005) 245 [[hep-ph/0508055](#)].
- [63] S. Moch, J. A. M. Vermaseren and A. Vogt, *The Quark form-factor at higher orders*, *JHEP* **08** (2005) 049 [[hep-ph/0507039](#)].
- [64] P. A. Baikov, K. G. Chetyrkin, A. V. Smirnov, V. A. Smirnov and M. Steinhauser, *Quark and gluon form factors to three loops*, *Phys. Rev. Lett.* **102** (2009) 212002 [[0902.3519](#)].
- [65] T. Gehrmann, E. W. N. Glover, T. Huber, N. Ikizlerli and C. Studerus, *Calculation of the quark and gluon form factors to three loops in QCD*, *JHEP* **06** (2010) 094 [[1004.3653](#)].
- [66] T. Gehrmann and D. Kara, *The $Hb\bar{b}$ form factor to three loops in QCD*, *JHEP* **09** (2014) 174 [[1407.8114](#)].
- [67] S. Moch, J. A. M. Vermaseren and A. Vogt, *The Three loop splitting functions in QCD: The Nonsinglet case*, *Nucl. Phys. B* **688** (2004) 101 [[hep-ph/0403192](#)].
- [68] A. Vogt, S. Moch and J. A. M. Vermaseren, *The Three-loop splitting functions in QCD: The Singlet case*, *Nucl. Phys. B* **691** (2004) 129 [[hep-ph/0404111](#)].
- [69] J. Blümlein, P. Marquard, C. Schneider and K. Schönwald, *The three-loop unpolarized and polarized non-singlet anomalous dimensions from off shell operator matrix elements*, *Nucl. Phys. B* **971** (2021) 115542 [[2107.06267](#)].
- [70] V. V. Sudakov, *Vertex parts at very high-energies in quantum electrodynamics*, *Sov. Phys. JETP* **3** (1956) 65.
- [71] A. H. Mueller, *On the Asymptotic Behavior of the Sudakov Form-factor*, *Phys. Rev. D* **20** (1979) 2037.
- [72] J. C. Collins, *Algorithm to Compute Corrections to the Sudakov Form-factor*, *Phys. Rev. D* **22** (1980) 1478.

- [73] A. Sen, *Asymptotic Behavior of the Sudakov Form-Factor in QCD*, *Phys. Rev. D* **24** (1981) 3281.
- [74] G. F. Sterman, *Summation of Large Corrections to Short Distance Hadronic Cross-Sections*, *Nucl. Phys. B* **281** (1987) 310.
- [75] S. Catani and L. Trentadue, *Resummation of the QCD Perturbative Series for Hard Processes*, *Nucl. Phys. B* **327** (1989) 323.
- [76] S. Catani and L. Trentadue, *Comment on QCD exponentiation at large x* , *Nucl. Phys. B* **353** (1991) 183.
- [77] N. Kidonakis and G. F. Sterman, *Resummation for QCD hard scattering*, *Nucl. Phys. B* **505** (1997) 321 [[hep-ph/9705234](#)].
- [78] N. Kidonakis, *A Unified approach to NNLO soft and virtual corrections in electroweak, Higgs, QCD, and SUSY processes*, *Int. J. Mod. Phys. A* **19** (2004) 1793 [[hep-ph/0303186](#)].
- [79] V. Ravindran, *On Sudakov and soft resummations in QCD*, *Nucl. Phys. B* **746** (2006) 58 [[hep-ph/0512249](#)].
- [80] V. Ravindran, *Higher-order threshold effects to inclusive processes in QCD*, *Nucl. Phys. B* **752** (2006) 173 [[hep-ph/0603041](#)].
- [81] S. Moch, J. A. M. Vermaseren and A. Vogt, *Higher-order corrections in threshold resummation*, *Nucl. Phys. B* **726** (2005) 317 [[hep-ph/0506288](#)].
- [82] E. Laenen and L. Magnea, *Threshold resummation for electroweak annihilation from DIS data*, *Phys. Lett. B* **632** (2006) 270 [[hep-ph/0508284](#)].
- [83] N. Kidonakis, *Next-to-next-to-next-to-leading-order soft-gluon corrections in hard-scattering processes near threshold*, *Phys. Rev. D* **73** (2006) 034001 [[hep-ph/0509079](#)].
- [84] A. Idilbi, X.-d. Ji and F. Yuan, *Resummation of threshold logarithms in effective field theory for DIS, Drell-Yan and Higgs production*, *Nucl. Phys. B* **753** (2006) 42 [[hep-ph/0605068](#)].
- [85] S. Catani, D. de Florian, M. Grazzini and P. Nason, *Soft gluon resummation for Higgs boson production at hadron colliders*, *JHEP* **07** (2003) 028 [[hep-ph/0306211](#)].
- [86] P. Banerjee, G. Das, P. K. Dhani and V. Ravindran, *Threshold resummation of the rapidity distribution for Drell-Yan production at NNLO+NNLL*, *Phys. Rev. D* **98** (2018) 054018 [[1805.01186](#)].
- [87] P. Banerjee, G. Das, P. K. Dhani and V. Ravindran, *Threshold resummation of the rapidity distribution for Higgs production at NNLO+NNLL*, *Phys. Rev. D* **97** (2018) 054024 [[1708.05706](#)].
- [88] T. Ahmed, A. H. Ajjath, G. Das, P. Mukherjee, V. Ravindran and S. Tiwari, *Soft-virtual correction and threshold resummation for n -colorless particles to fourth order in QCD: Part I*, [2010.02979](#).
- [89] B. Ruijl, T. Ueda and J. A. M. Vermaseren, *FORM version 4.2*, [1707.06453](#).
- [90] S. Catani, M. L. Mangano, P. Nason and L. Trentadue, *The Resummation of soft gluons in hadronic collisions*, *Nucl. Phys. B* **478** (1996) 273 [[hep-ph/9604351](#)].
- [91] A. Vogt, *Efficient evolution of unpolarized and polarized parton distributions with QCD-PEGASUS*, *Comput. Phys. Commun.* **170** (2005) 65 [[hep-ph/0408244](#)].

- [92] NNPDF collaboration, R. D. Ball et al., *Parton distributions from high-precision collider data*, *Eur. Phys. J. C* **77** (2017) 663 [1706.00428].
- [93] A. Buckley, J. Ferrando, S. Lloyd, K. Nordström, B. Page, M. Rüfenacht et al., *LHAPDF6: parton density access in the LHC precision era*, *Eur. Phys. J. C* **75** (2015) 132 [1412.7420].
- [94] M. Grazzini, S. Kallweit and M. Wiesemann, *Fully differential NNLO computations with MATRIX*, *Eur. Phys. J. C* **78** (2018) 537 [1711.06631].
- [95] J. Alwall, M. Herquet, F. Maltoni, O. Mattelaer and T. Stelzer, *Madgraph 5: going beyond*, *Journal of High Energy Physics* **2011** (2011) .
- [96] F. Cascioli, T. Gehrmann, M. Grazzini, S. Kallweit, P. Maierhöfer, A. von Manteuffel et al., *ZZ production at hadron colliders in NNLO QCD*, *Phys. Lett. B* **735** (2014) 311 [1405.2219].
- [97] M. Grazzini, S. Kallweit and D. Rathlev, *ZZ production at the LHC: fiducial cross sections and distributions in NNLO QCD*, *Phys. Lett. B* **750** (2015) 407 [1507.06257].
- [98] A. A H, A. Chakraborty, G. Das, P. Mukherjee and V. Ravindran, *Resummed prediction for Higgs boson production through $b\bar{b}$ annihilation at N^3LL* , *JHEP* **11** (2019) 006 [1905.03771].
- [99] A. A H, G. Das, M. C. Kumar, P. Mukherjee, V. Ravindran and K. Samanta, *Resummed Drell-Yan cross-section at N^3LL* , *JHEP* **10** (2020) 153 [2001.11377].
- [100] A. A H, P. Mukherjee and V. Ravindran, *Next to soft corrections to Drell-Yan and Higgs boson productions*, *Phys. Rev. D* **105** (2022) 094035 [2006.06726].
- [101] A. A H, P. Mukherjee, V. Ravindran, A. Sankar and S. Tiwari, *Next-to SV resummed Drell-Yan cross section beyond leading-logarithm*, *Eur. Phys. J. C* **82** (2022) 234 [2107.09717].
- [102] A. A H, P. Mukherjee, V. Ravindran, A. Sankar and S. Tiwari, *Resummed Higgs boson cross section at next-to SV to NNLO + \overline{NNLL}* , *Eur. Phys. J. C* **82** (2022) 774 [2109.12657].
- [103] A. Bhattacharya, M. C. Kumar, P. Mathews and V. Ravindran, *Next-to-soft-virtual resummed prediction for pseudoscalar Higgs boson production at NNLO+NNLL $^-$* , *Phys. Rev. D* **105** (2022) 116015 [2112.02341].
- [104] V. Ravindran, A. Sankar and S. Tiwari, *Resummed next-to-soft corrections to rapidity distribution of Higgs boson to NNLO+NNLL $^-$* , *Phys. Rev. D* **108** (2023) 014012 [2205.11560].
- [105] G. Das, C. Dey, M. C. Kumar and K. Samanta, *Precision Studies for Higgs-Strahlung Process at Hadron Collider*, *Springer Proc. Phys.* **304** (2024) 245.
- [106] P. Banerjee, C. Dey, M. C. Kumar and V. Pandey, *Threshold Resummation for Z-boson Pair Production*, *Acta Phys. Polon. Supp.* **18** (2025) .
- [107] G. Das, C. Dey, M. C. Kumar and K. Samanta, *Soft gluon resummation for gluon fusion ZH production*, **2501.10330**.
- [108] A. Bhattacharya, C. Dey, M. C. Kumar and V. Pandey, *Next to Soft Threshold Resummation for VH Production*, **2502.20331**.
- [109] P. Banerjee, *Threshold resummation for ZZ production*, **3**, 2025, **2503.00512**.

- [110] F. Caola, M. Dowling, K. Melnikov, R. Röntsch and L. Tancredi, *QCD corrections to vector boson pair production in gluon fusion including interference effects with off-shell Higgs at the LHC*, *JHEP* **07** (2016) 087 [[1605.04610](#)].
- [111] J. M. Henn, M. Stahlhofen, M. Steinhauser and M. Wormser, *Matter dependence of the four-loop QCD cusp anomalous dimension: from small angles to all angles*, *JHEP* **04** (2020) 003 [[1911.10174](#)].
- [112] T. Huber, T. Hurth, E. Lunghi and J. Virto, *Logarithmically Enhanced Contributions to the Angular Observables in $B \rightarrow V\ell\ell$* , *JHEP* **08** (2019) 152 [[1905.00965](#)].
- [113] A. von Manteuffel, R. M. Schabinger and H. X. Zhu, *The two-loop soft function for heavy quark pair production at future linear colliders*, *JHEP* **08** (2020) 068 [[2003.01798](#)].